

DOI 10.24425/ae.2021.136061

The slewing drive system for tower crane with permanent magnet synchronous motor

ŁUKASZ KNYPÍŃSKI , JACEK KRUPIŃSKI*Poznan University of Technology
Poland**Krupiński Cranes
Poland**e-mail: lukasz.knypinski@put.poznan.pl*

(Received: 02.08.2020, revised: 02.10.2020)

Abstract: The paper presents a method of determining the efficiency of the slewing drive system applied in tower cranes. An algorithm for the proper selection of a permanent magnet synchronous motor (PMSM) for crane applications is presented. In the first stage of our research the proper PMSM was proposed on the basis of the simulation calculation. Next, the PM motor was examined on a special test bench. The experimental setup allows determining major electrical and mechanical parameters of the motor drive system. The applied slewing system consists of: an inverter, gear, cable drum and a permanent magnet motor. The performance and efficiency of the system were experimentally determined. Selected results of the experimental measurement are presented and discussed.

Key words: energy conversion efficiency, permanent magnet synchronous motor, slewing drive system, system efficiency, tower cranes

1. Introduction

Nowadays, electricity is used in almost all production processes. The major part of electricity is consumed by electrical machines, mainly, this involves the processing of electricity into mechanical energy by electrical motors [1]. Nowadays, induction motors are used most frequently [2, 3]. The mathematical model of phenomena in induction motors is well known [4, 5]. They are commonly used in the construction industry and mining industry as drives of industrial machine tools, and also in agriculture and consumer equipment. The currently manufactured



© 2021. The Author(s). This is an open-access article distributed under the terms of the Creative Commons Attribution-NonCommercial-NoDerivatives License (CC BY-NC-ND 4.0, <https://creativecommons.org/licenses/by-nc-nd/4.0/>), which permits use, distribution, and reproduction in any medium, provided that the Article is properly cited, the use is non-commercial, and no modifications or adaptations are made.

induction motors and even high-efficiency induction motors are characterized by low values of functional parameters in relation to the latest designs of permanent magnet (PM) motors [6–15].

Quickly developing global economy and more and more rigorous requirements regarding the energy consumption force designers to look for new, better and more efficient designs of electrical motors. One of the most energy-consuming fields of economy is the construction industry in which cranes are used commonly. In accordance with the catalogue data, the power of all motors installed in the crane ranges between 15–35 kW [26], depending on the crane type.

There are different types of electrical motors used in crane drive systems. Most frequently, these are induction motors powered by inverters. The type of the used electrical motor is strictly associated with the intended use of the device. In addition to the proper selection of the drive motor in the crane system, the control system, which significantly affects the energy processing efficiency in the entire drive system, is an important element. In the case of estimating the energy consumption of the drive for cranes, it is necessary to determine the efficiency of not only the motor, but the entire drive system [16]. Also, in this case, the selection of the proper control system strictly depends on the intended use of the crane. The most important requirement set for manufacturers of crane systems is a guarantee of a high level of safety for their users.

In this paper, the conversion efficiency of the slewing drive system based on the permanent magnet synchronous motor for a tower crane is presented. The algorithm of proper PM motor selection for crane applications is introduced in Section 2. The construction of a special test bench for the investigation of the slewing drive system is shown in Section 3. Next, the results of experimental measurements of the PM synchronous motor and slewing propulsion system are presented in Section 4. The comparison of energy conversion efficiency for all propulsion systems applied in the tower crane is presented in Section 5. The conclusions and discussion about future work are included in Section 6.

2. Algorithm of the PM motor selection to crane applications

The computer software to determine the static point of work of the motor was developed. This software used an analytical model of the propulsion system in the Delphi 7.0 environment. The input data are the catalog data of the motor and the shape of the motion profile. The diagram of the drive system that consists of: (a) a motor, (b) a gear, (c) a cable drum and (d) a load, is shown in Fig. 1.

The rms (T_{rms}) and maximum (T_{max}) value of torque on the motor shaft can be expressed as follows:

$$T_{\text{rms}} = F_{\text{rms}} \left(\frac{D_b}{2i_d i_g \eta_d \eta_g} \right) + T_{d \text{ rms}}, \quad (1)$$

$$T_{\text{max}} = F_{\text{max}} \left(\frac{D_b}{2i_d i_g \eta_d \eta_g} \right) + T_{d \text{ max}}, \quad (2)$$

where: F_{max} is the maximum resistance force, F_{rms} is the rms resistance force of the system, D_b is the cable drum diameter, i_d is the cable drum transmission, i_g is the gear ratio, η_d is the cable drum efficiency, η_g is the transmission efficiency, $T_{d \text{ rms}}$ is the rms value of a dynamic moment, $T_{d \text{ max}}$ is the maximum value of a dynamic moment.

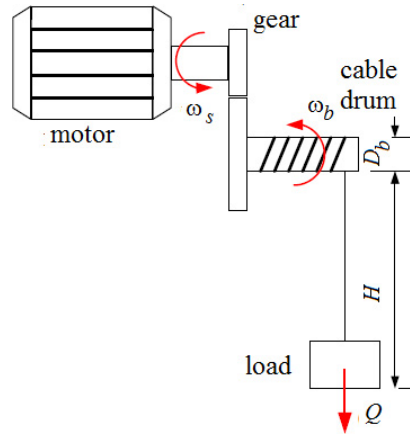


Fig. 1. Schematic view of propulsion system for crane application

In the developed algorithm, the values of dynamic moments are calculated according to the following formulas [18]:

$$T_{d\text{ rms}} = J\varepsilon_{\text{rms}}, \quad (3)$$

$$T_{d\text{ max}} = J\varepsilon_{\text{max}}, \quad (4)$$

where: J is the moment of inertia of rotational mass brought down to the motor shaft, ε_{rms} is the rms angular acceleration, ε_{max} is the maximum angular acceleration of the motor.

The moment of inertia of the rotating mass brought down to the motor shaft in the adopted crane system is determined as:

$$J = J_s + J_g + \frac{J_b}{(\eta_g i_g)^2}, \quad (5)$$

where: J_s is the moment of inertia of the PM motor, J_g is the moment of inertia of the gear, J_b is the moment of inertia of the cable drum.

In order to determine dynamic moments ($T_{d\text{ rms}}$, $T_{d\text{ max}}$), the motion profile of a duty cycle must be taken into account. The trapezoidal motion profile has been taken into account in the developed computational algorithm (see Fig. 2) [17]. In such a case the values of the angular acceleration can be determined as:

$$\varepsilon_{\text{max}} = \frac{1}{t_a} \left(\frac{2i_d v}{D_b} \right), \quad (6)$$

$$J = J_s + J_g + \frac{J_b}{(\eta_g i_g)^2}, \quad (7)$$

where: v is the maximum linear speed of the lifted load, $t_t = t_a + t_r + t_c + t_b$ is the total duration of the work cycle, t_a is the acceleration time, t_r is the time of work with the constant speed, t_c is the braking time, t_b is the break time.

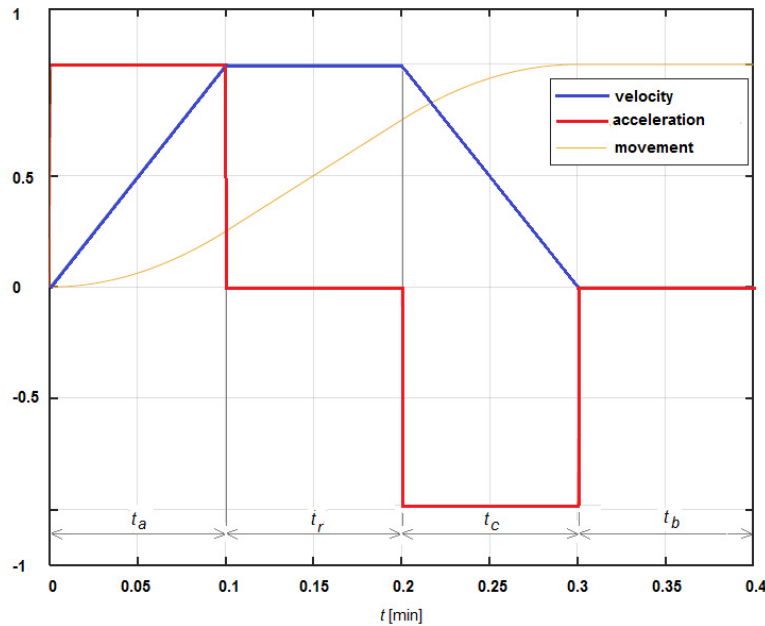


Fig. 2. The trapezoidal motion profile, t_a is the acceleration time, t_r is the time of work with constant speed, t_c is the braking time, t_b is the break time

The maximum resistance force for the adopted drive system can be derived:

$$F_{\max} = F_r + m_t \left(g + \frac{v}{t_a} \right), \quad (8)$$

where: F_r is the friction force, g is the gravitational acceleration, m_t is the total mass, consisting of the weight of the lifted load and additional mass, i.e. rope mass, declared before the start of the calculation.

The value of the rms resistance force was determined using the equation:

$$F_{\text{rms}} = \sqrt{\frac{t_m (g m_t + F_r)^2 + t_a \left(\frac{m_t v}{t_a} \right)^2 - t_c \left(\frac{m_t v}{t_a} \right)^2}{t_t}}, \quad (9)$$

in which t_m is the time of load lifting.

The maximum mechanical power on the shaft of the motor can be determined using Equation (2), i.e. [19]:

$$P_{\max} = T_{\max} i_g \left(\frac{2i_b v}{D_b} \right). \quad (10)$$

Moreover, the rms mechanical (output) power on the motor shaft is determined as:

$$P_{\text{rms}} = T_{\text{rms}} \left(\frac{2i_b i_g v}{D_b} \right). \quad (11)$$

The value of the maximum electrical (input) motor power $P_{s \max}$ and the rms motor power $P_{s \text{rms}}$ can be obtained by:

$$P_{s \max} = P_{\max} + \chi \Delta P_{cu \max}, \quad (12)$$

$$P_{s \text{rms}} = P_{\text{rms}} + \chi \Delta P_{cu \text{rms}}, \quad (13)$$

where: χ is the loss factor, $\Delta P_{cu \max}$ is the maximum losses in copper, $\Delta P_{cu \text{rms}}$ represents the rms losses in the copper.

Based on the above algorithm, a preliminary estimation of the functional parameters of PM synchronous motors for all drives applied in the constructed tower crane has been made.

2.1. The rated parameters of the motor for the slewing drive system

Using the presented algorithm, the type of motors for all drives for the designed tower crane was selected. The rated parameter of motors for the trolley travelling drive was presented in [17]. In the case of the slewing drive, the Beckhoff AM 8063-3N40 was proposed. Table 1 contains the rated parameters of the motor for the slewing drive system.

Table 1. The rated parameters of the Beckhoff AM 8063-3N40 motor

Parameter	Unit	Value
Rated torque	Nm	13.2
Peak torque	Nm	111
Standstill torque	Nm	29
Rated power	kW	4.15
Rated speed	rpm	3000
Maximum value of line voltage	V	480
Number of poles	–	10
Rotor moment of inertia	kgcm ²	29
Standstill current	A	17.2
Peak current	A	80.9

2.2. Determining the best shape of the motion profile

The elaborated software is equipped with an optimization module. The optimization module contains the classical particle swarm optimization (PSO) method [7, 20]. The optimization module allows determining the parameters of the trapezoidal motion profile for which electricity consumption is minimal for the assumed profile, depending on the assigned rated parameters of the motor. This module is not available for the person using the crane device.

3. The experimental test bench setup

In order to verify the proper selection of the motor, a test bench for experimental investigation of properties of a PMSM was constructed. The test bench consists of: (a) a channel power analyzer, (b) a main filter, (c) a power inverter, (d) the tested PM synchronous motor and (d) an active load system. The block diagram of the experimental test bench is presented in Fig. 3. The experimental bench is automated and computer-controlled. All the measured electrical parameters and mechanical parameters are saved into CSV files and are used to determine electrical and mechanical propulsion system parameters.

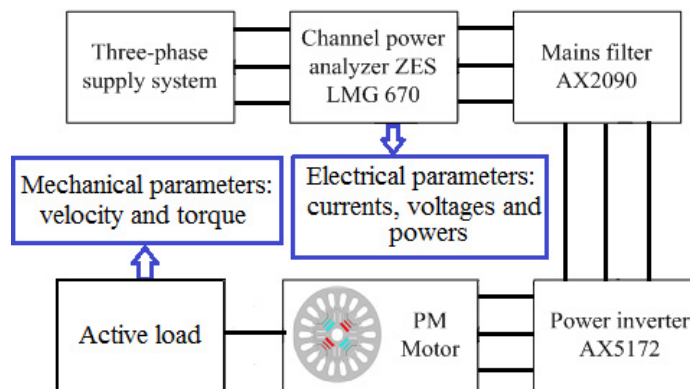


Fig. 3. The block diagram of the test bench setup

The active load system with a dynamometer is also computer-controlled, it allows free modeling of the load characteristic. It is possible to set a motion profile with the desired shapes and accelerations. The configuration of the experimental setup is presented in Fig. 4.

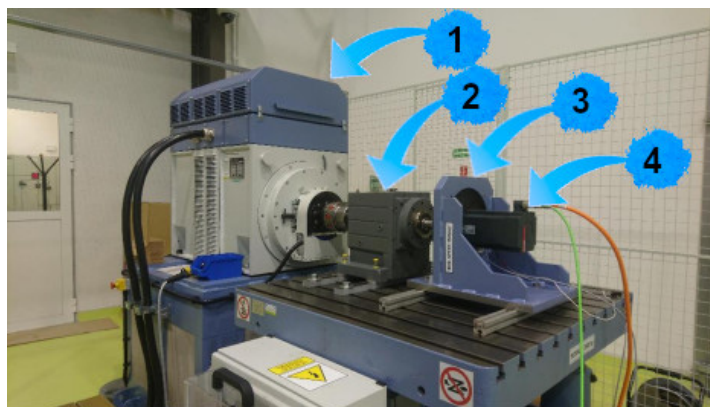


Fig. 4. The view of experimental bench for examination of the slewing drive system properties: 1 – active load system with dynamometer; 2 – gear; 3 – flange mount for motor; 4 – PM synchronous motor

4. The experimental test of motor and the propulsion system

The main aim of the measurements was the estimation of properties of the examined slewing drive system. The most important task is the calculation of the energy conversion efficiency in the slewing drive system. All the measurements of mechanical and electrical quantities were performed in the test bench setup presented above.

4.1. Measurements of the PMSM in no-load condition

In the first test the back-electromotive force (EMF) was measured. The examined motor was propelled with a rotational speed of 1400 rpm. The waveforms of the back-EMF in the specific phases are shown in Fig. 5(a). Fig. 5(b) shows the spectrum of harmonic of the back-EMF in the track of the first phase of the motor. The rms value of the phase back-EMF is equal to 221.3 V. Thus, the maximum value is 321.9 V.

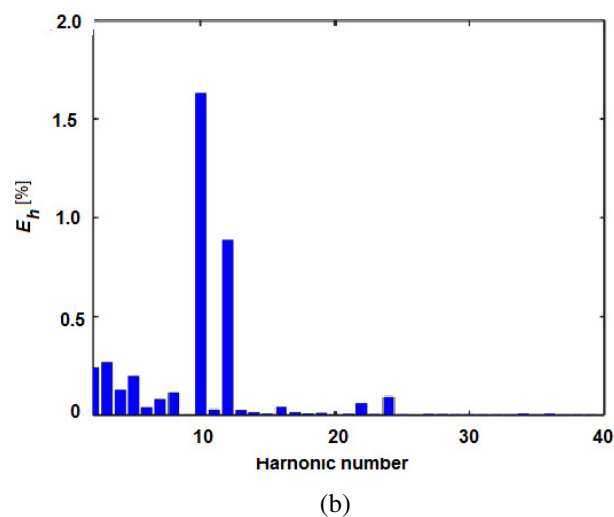
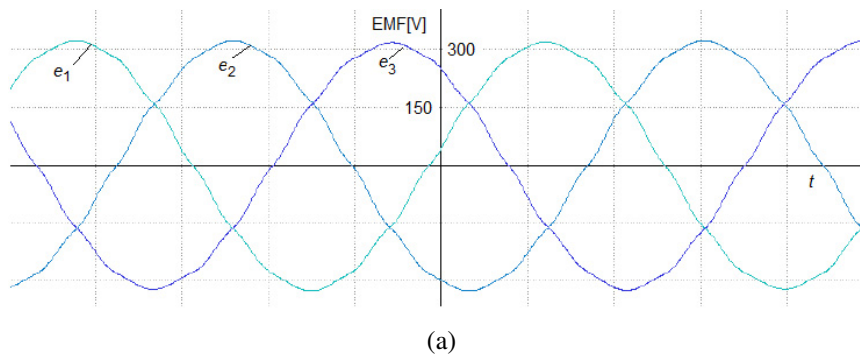


Fig. 5. Results of the measurement in no-load condition: (a) back-EMF waveforms; (b) spectrum of harmonics of back-EMF in the first phase of the motor

During the measurements, the THD coefficient for the first phase equaled 1.83%. One can observe the significant influence on the value of the THD coefficient for the 10th and 12th harmonics, which were valued correspondingly as 1.63% and 0.91%, respectively.

4.2. Measurements of the propulsion system properties in load condition

Next, the measurements were taken for the slewing drive system under the workload condition. The results of the measurement in the assigned motion profile are shown in Fig. 6.

The work of the drive was modeled with the trapezoidal profile of the movement. During the experimental research the characteristic times were assumed: the acceleration time t_a , the braking time t_c and the time of work with the constant velocity t_r . All three times were identical and equaled 15 seconds. The break-time t_b was equal to 30 seconds. The following mechanical parameters were assumed: the maximum rotational velocity equaled 1 560 rpm, the maximum loading torque $T_l = 37$ Nm.

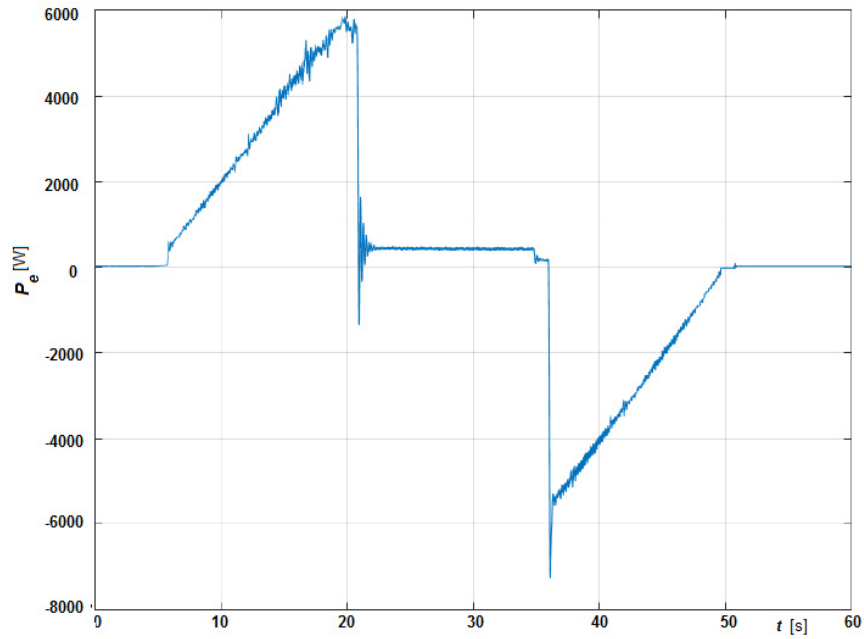
The maximum temporary value of the electric power consumed by the drive system from the supply network was $P_e = 5.9$ kW during the acceleration process, whereas the temporary value for the braking stage was $P_e = 7.2$ kW (see Fig. 6(a)). The test results were the basis of estimating the median value of electromagnetic torque produced by the motor, which was $T = 35$ Nm (see Fig 6(b)).

On the basis of the obtained measurements results, it can be observed that the greatest value of electromagnetic torque is achieved during start-up of the slewing drive system. In this state, the drive system has to overcome a large value of the moment of inertia. During the period of work with constant speed, the value of electromagnetic torque is much lower. In the case of the acceleration period, the velocity increases linearly, the mechanical energy is supplied to the driven system.

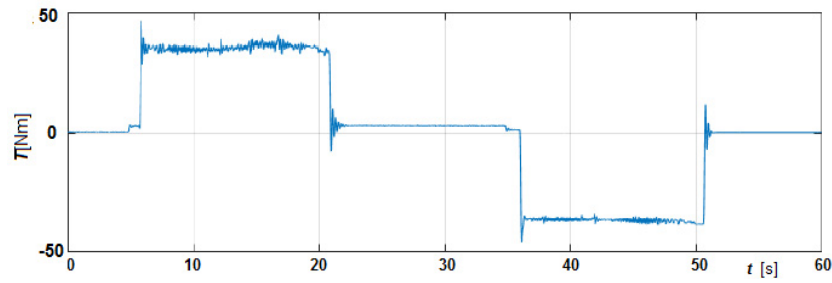
The obtained test results of electrical and mechanical quantities were used to define the rms values of voltage and rms values of currents in the specific phases of the analyzed drive system. Additionally, the active power for each phase during the working cycle and the power factor were also estimated. The results of the measurements are presented in Table 2.

Table 2. The determined electrical parameters of the slewing drive system

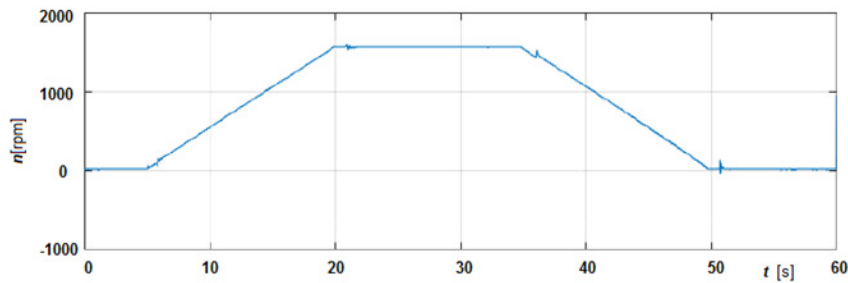
Parameter	Unit	Phase 1	Phase 2	Phase 3
RMS voltage	V	230.1	232.1	229.4
Voltage THD coefficient	%	1.83	1.82	2.01
RMS current	A	10.374	11.018	11.167
Current THD coefficient	%	99.1	101.2	100.4
Active electric power	W	1381	1381	1379
Power factor	–	0.66	0.64	0.63



(a)



(b)



(c)

Fig. 6. The mechanical and electrical waveforms during enforced work cycle: (a) the electric power waveform; (b) the loading waveform and (c) the velocity waveform

The value of the slewing drive efficiency was calculated with the use of mechanical and electrical values for all the phases [20, 21] and was determined as:

$$\eta = \frac{P_{\text{rms}}}{P_{s \text{ rms}}} 100, \quad (14)$$

For the researched system the value of the energy conversion efficiency equaled 87.982%.

The spectrum of the harmonic content of supply current before the power inverter fed the slewing drive system (see Fig. 3) was analyzed. The harmonic content of the current of the first phase is shown in Fig. 7.

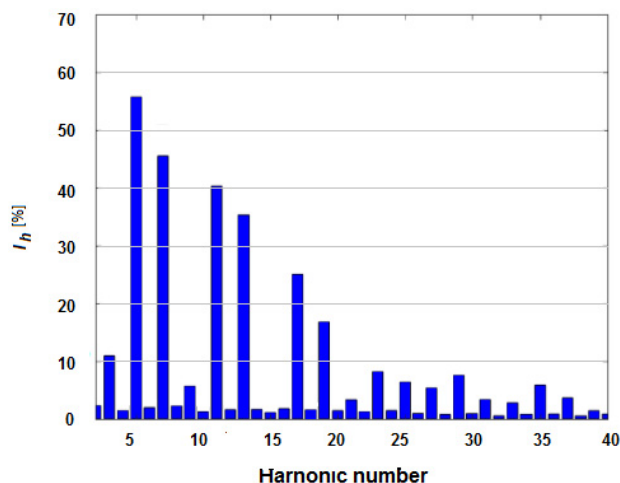


Fig. 7. The spectrum of harmonics of the current in the first phase

The analysis showed a high value of the THD coefficient for the supply current. In the case of supplying PMSMs by inverter-equipped systems one usually observes a high content of odd harmonics, that is 5, 7, 11 and 13 [22–25].

5. Comparison of the properties of all drive systems used in the designed tower crane

The aim of our research was to evaluate the possibility of the application of drive systems based on permanent magnet synchronous motors in the construction of tower cranes. The designed tower crane will be equipped with following drive systems: (a) the hoist winch drive, (b) the trolley travelling drive and (c) the slewing drive. The PMSMs for all propulsion systems were selected using the algorithm presented in the second section of the article. The performance parameters of all propulsion systems were investigated on the experimental test bench setup [17, 21]. The comparison of functional parameters for all the tested drives systems is shown in Table 3.

Based on the presented measurement results, it can be noted that the best parameters were obtained for the hoist winch drive, both the efficiency and the power factor value. The worst

Table 3. Comparison of electrical parameters of propulsion systems

Type of drive	Efficiency	Power factor	Voltage THD
	%	–	%
Hoist winch drive	88.045	0.753	1.71
Trolley travelling drive	73.895	0.605	1.46
Slewing drive	87.982	0.643	1.886

performance was obtained for the trolley travelling drive. In the case of the trolley travelling drive, the position of the trolley is controlled by a system of ropes moving on rollers. For this type of drive, the good dynamic of movement is more important than the energetic efficiency. Often, a higher power of an inverter is applied to compensate for load fluctuations caused by the movement of the swinging load and weather conditions.

6. Conclusions

This paper presents an algorithm for the correct choice of a PM synchronous motor for the drive system used in cranes' applications. Employing this algorithm, the PM motors for the following systems were chosen: (a) the hoist winch drive, (b) the trolley traveling drive, (c) the slewing drive. The functional parameters of each motor drive were measured on the built test bench. The taken measurements allowed calculating the efficiencies of each drive. The energy conversion efficiency obtained during our investigation is encouraging. As a result, the following efficiency for propulsion systems were obtained: (a) the hoist winch drive equals 88.045%, (b) slewing drive equals 87.982% and (c) the trolley travelling drive equals 73.895%. At present, the prototype of a tower crane equipped with PM motors is being constructed. The efficiency of the tower cranes equipped with PM synchronous motors will be compared with the efficiency of the cranes equipped with conventional induction motors.

The next research will focus on developing a new construction of the hoist winch motor, where the rotor would be directly coupled with the drum for line winding. In such a drive system there would be no need for a gear, which makes the construction less complicated and thus reduces the production and operating cost. A project of such a new machine will be determined with the use of the newest non-deterministic optimization procedures.

Acknowledgements

This work was supported by the National Center of Research and Developments of Poland under Project POIR.01.01.01-00-1220/17.

References

- [1] Gansen A.U., Chokkalingam L.N., *Self-start synchronous reluctance motor new rotor designs and its performance characteristic*, International Transaction on Electrical Energy Systems, vol. 29, no. 11, pp. 1–22 (2019).

- [2] Resa J., Cortes D., Marquez-Rubio J.F., Navarro D., *Reduction of induction motor energy consumption via variable velocity and flux references*, Electronics, vol. 8, no. 740, pp. 1–14 (2019).
- [3] Belmans R., Bisschots F., Trimmer R., *Practical design considerations for braking problems in overhead crane drives*, Annual Meetings of IEEE Industry Applications Society – IAS, vol. 1, pp. 473–479 (1993).
- [4] Barański M., *FE analysis of coupled electromagnetic-thermal phenomena in the squirrel cage motor working at high ambient temperature*, COMPEL, vol. 38, no. 4, pp. 1120–1132 (2019).
- [5] Kometani H., Sakabe S., Nakanishi K., *3-D electro-magnetic analyses of a cage induction motor with rotor skew*, IEEE Transactions on Energy Conversion, vol. 11, no. 2, pp. 331–337 (1996).
- [6] Torrent M., Perat J.I., Jimenez J.A., *Permanent magnet synchronous motor with different rotor structures for traction motor in high speed trains*, Energies, vol. 11, no. 1549, pp. 1–17 (2018).
- [7] Knypiński Ł., Nowak L., Demenko A., *Optimization of the synchronous motor with hybrid permanent magnet excitation system*, COMPEL, 2015, vol. 34, no. 2, pp. 448–455 (2015).
- [8] Zawilak T., *Influence of rotor's cage resistance on demagnetization process in the line start permanent magnet synchronous motor*, Archives of Electrical Engineering, vol. 69, no. 2, pp. 249–258 (2020).
- [9] Knypiński Ł., Pawełoszek K., Le Manech Y., *Optimization of low-power line-start PM motor using gray wolf metaheuristic algorithm*, Energies, vol. 13, no. 5, pp. 1–11 (2020).
- [10] Dorell D.G., Popescu M., Evans L., Staton D.A., Knight A.M., *Comparison of the permanent magnet drive motor with a cage induction motor design for a hybrid electric vehicle*, Proceedings of International Power Electronics Conference – ICCE ASIA, pp. 1–6 (2010), DOI: [10.1109/IPEC.2010.5543566](https://doi.org/10.1109/IPEC.2010.5543566).
- [11] Barański M., Szeląg W., Łyskawiński W., *An analysis of a start-up process in LSPMSMs with aluminum and copper rotor bars considering the coupling of electromagnetic and thermal phenomena*, Archives of Electrical Engineering, vol. 68, no. 4, pp. 933–946 (2019).
- [12] Ślusarek B., Kapelski D., Antal L., Zalas P., Gwozdziejewicz M., *Synchronous motor with hybrid permanent magnets on the rotor*, Sensors, vol. 14, pp. 12425–12436 (2014).
- [13] Jedryczka C., Szeląg W., Piech J., *Multiphase permanent magnet synchronous motors with fractional slot windings*, COMPEL, vol. 35, no. 6, pp. 1937–1948 (2016).
- [14] Wardach M., Pałka R., Paplicki P., Bronisławski M., *Novel hybrid excited machine with flux barriers in rotor structure*, COMPEL, vol. 37, no. 4, pp. 1489–1499 (2018).
- [15] Młynarek P., Łukaniszyn M., Jagieła M., Kowol M., *Modelling of heat transfer in low-power IPM synchronous motors*, IET Science, Measurement and Technology, vol. 12, no. 8, pp. 1066–1073 (2018).
- [16] Rebelo J.M., Silvestre M.A.R., *Development of a coreless permanent magnet synchronous motor for a battery electric shell eco marathon prototype vehicle*, Open Engineering, vol. 8, no. 1, pp. 382–390 (2018).
- [17] Knypiński Ł., Krupiński J., *The energy conversion efficiency in the trolley travelling drive system in tower cranes*, Proceedings of 15-th Selected Issue of Electrical Engineering and Electronics – WZEE, pp. 1–4 (2020), DOI: [10.1109/WZEE48932.2019.8979940](https://doi.org/10.1109/WZEE48932.2019.8979940).
- [18] Egrov A., Kozlow K., Belogusev V., *Method for evaluation of the chain derive efficiency*, Journal of Applied Engineering Science, vol. 341, pp. 277–282 (2015).
- [19] Janaszek M., *The analysis of the influence unequal parameters of motors on the work of multimotors traction drive*, Journal of the Electrical Engineering Institute (in Polish), vol. 286, pp. 1–26 (2015).
- [20] Dambrauskas K., Vanagas J., Zimnickas T., Kalvaitisand A., Ažubalis K., *A method for efficiency determination of permanent magnet synchronous motor*, Energies, vol. 13, no. 1004, pp. 1–15 (2020).

- [21] Knypiński Ł., Krupiński J., *Application of the permanent magnet synchronous motors for tower cranes*, Przegląd Elektrotechniczny, vol. 96, no. 1, pp. 27–30 (2020), DOI: [10.15199/48.2020.01.07](https://doi.org/10.15199/48.2020.01.07).
- [22] Geng S., Zhang Y., Qiu H., Yang R., Yi R., *Influence of harmonic voltage coupling on torque ripple of permanent magnet synchronous motor*, Archives of Electrical Engineering, vol. 68, no. 2, pp. 399–410 (2019).
- [23] Dong S., Zhang Q., Ma H., Wang R., *Design for the interior permanent magnet synchronous motor drive system based on the Z-source inverter*, Energies, vol. 12, no. 3350, pp. 1–14 (2019).
- [24] Chen Z., Zhang H., Tu W., Luo G., Manoharan D., Kennel R., *Sensorless control for permanent magnet synchronous motor in rail transient applications using segmented synchronous modulation*, IEEE Access, vol. 7, pp. 76669–7667 (2019).
- [25] Putz Ł., Bednarek K., Kasprzyk L., *Analysis of higher harmonics generated by LED lamps*, Przegląd Elektrotechniczny, vol. 96, no. 4, pp. 90–93 (2020).
- [26] <https://www.krupinskichcranes.com>, accessed July 2020.